Published in final edited form as:
J Phys Chem B. 2008 November 13; 112(45): 14312–14318. doi:10.1021/jp805952w.

Anesthetic modulation of protein dynamics: insights from a NMR study

Christian G. Canlas[1], **Tanxing Cui**[1], **Ling Li**[1], **Yan Xu**[1,2], and **Pei Tang**[1,2,3,*]

1*Department of Anesthesiology, University of Pittsburgh School of Medicine, Pittsburgh, PA 15261*

2*Department of Pharmacology, University of Pittsburgh School of Medicine, Pittsburgh, PA 15261*

3*Department of Computational Biology, University of Pittsburgh School of Medicine, Pittsburgh, PA 15261*

Abstract

Mistic (Membrane Integrating Sequence for Translation of Integral Membrane Protein Constructs) comprises the four-α-helix bundle scaffold found in the transmembrane domains of the Cys-loop receptors that are plausible targets for general anesthetics. Nuclear magnetic resonance (NMR) studies of anesthetic halothane interaction with Mistic in dodecyl phosphocholine (DPC) micelles provide an experimental basis for understanding molecular mechanisms of general anesthesia. Halothane was found to interact directly with Mistic, mostly in the interfacial loop regions. Although the presence of halothane had little effect on Mistic structure, ^{15}N NMR relaxation dispersion measurements revealed that halothane affected Mistic's motion on the microsecond-millisecond timescale. Halothane shifted the equilibrium of chemical exchange in some residues and made the exchange faster or slower in comparison to the original state in the absence of halothane. The motion on the microsecond-millisecond timescale in several residues disappeared in response to the addition of halothane. Most of the residues experiencing halothane-induced dynamics changes also exhibited profound halothane-induced changes in chemical shift, suggesting that dynamics modification of these residues might result from their direct interaction with halothane molecules. Allosteric modulation by halothane also contributed to dynamics changes, as reflected in residues I52 and Y8 where halothane introduction brought about dynamics changes but not chemical shift changes. The study suggested that inhaled general anesthetics could act on proteins via altering protein motion on the microsecond-millisecond timescale, especially motion in the flexible loops that link different alpha helices. The validation of anesthetic effect on protein dynamics that are potentially correlated with protein functions is a critical step in unraveling the mechanisms of anesthetic action on proteins.

Keywords

mechanisms of general anesthesia; halothane; general anesthetic; protein-ligand interaction; NMR; protein dynamic

INTRODUCTION

The molecular mechanism of general anesthesia remains unsolved. The current consensus is that inhaled anesthetics act in the central nervous system and affect neural networks. A wealth of molecular biology and electrophysiology data has demonstrated that neurotransmitter gated ion channels, particularly Cys-loop receptors,[1,2] are plausible targets for general anesthetics.

*Send all correspondence to: Professor Pei Tang, Ph.D., 2049 Biomedical Science Tower 3, 3501 Fifth Avenue, University of Pittsburgh, Pittsburgh, Pennsylvania 15260, Tel (412) 383-9798, Fax (412) 648-8998, Email: E-mail: tangp@anes.upmc.edu.

These ion channels are sensitive to volatile anesthetics at clinically effective concentrations. The channel functions could be inhibited or potentiated significantly by general anesthetics in the excitatory (nicotinic acetylcholine and serotonin type 3) or inhibitory ($GABA_A$ and glycine) receptors, respectively.[1,2] It is, however, still debatable where anesthetic binding sites reside and whether the traditional lock-and-key-binding paradigm is applicable for anesthetics interacting with proteins. We have recently proposed a hypothesis of anesthetic action based on protein global dynamics[3] and contend that the *necessary* and *sufficient* condition for general anesthetics, as well as other low-affinity drugs, to exert their action on proteins is to disrupt the modes of motion essential to protein functions. Experimental evidence is critical to further validate the hypothesis in addition to computational studies.[3,4]

Directly obtaining information concerning anesthetic modulation on structures and dynamics of neuronal ion channels with atomic resolution is often prohibited by technical obstacles, such as limitations on protein size for NMR spectroscopy or challenges as regards crystallization of membrane proteins for x-ray crystallography. As an alternative approach, model proteins that mimic certain properties of neuronal ion channels have been used to understand the structural basis of anesthetic-protein interaction. Proteins of four-α-helix bundle structural motif are useful models because binding pockets of inhaled anesthetics are presumed to be within transmembrane four-α-helix bundles of Cys-loop receptors.[5] A de novo designed prototype four-α-helix bundle with specific anesthetic binding pockets[6–8] and a natural soluble four-α-helix bundle protein (ferritin)[9] served previously as models for investigating the structural basis of inhaled anesthetic binding in proteins with such a special structural motif. The knowledge gained from these studies could be applicable for understanding molecular insights of anesthetics in much more complex neurotransmitter gated ion channels.

Our recent NMR studies[7,8] on a water-soluble de novo designed prototype four-α-helix bundle indicated that motion of the four-α-helix bundle could be modulated by halothane, an inhaled general anesthetic. This inspired us to look into similar anesthetic effects on other four-α-helix bundle proteins and to investigate whether there are any common anesthetic effects on four-α-helix bundle proteins. Mistic was chosen for the present study because it could naturally fold into a four-α-helix bundle motif in micelles. The structure of this 110-amino acid (13 kD) *B. subtilis* protein was previously determined with NMR in lauryl dimethylamine oxide (LDAO) micelles.[10] High quality NMR spectra of Mistic allow for exploring molecular details of anesthetic and Mistic interaction at atomic resolution. Conformational flexibility of Mistic offers a possibility to assess potential structural and dynamical changes as a consequence of the interaction with halothane. The working hypothesis of our study on Mistic is that volatile general anesthetics act on proteins via altering protein motions, especially motions in the flexible loops which link different α helices.

MATERIALS AND METHODS

Sample Preparation

The gene encoded Mistic was cloned from the *Bacillus subtilis* into the expression vector pTBSG1 (a gift from Prof. Timothy A. Cross' laboratory at Florida State University). The Mistic was expressed in strain BL21(DE3) CodonPlus cells using the Marley protocol.[11] Typically the expression was induced with 0.2 mM IPTG and kept in M9 minimal medium at 12°C for about 80 hours. The protein was purified using the published procedures.[10] A yield of ~120 mg purified Mistic was obtained from each liter of M9 minimal media.

Mistic was insoluble in water. The presence of detergent is essential for solubilizing Mistic. Mistic is stable in lauryl dimethylamine oxide (LDAO) for ~5 days, but more than 5 months in dodecyl phosphocholine (DPC). The exchange of DPC for LDAO was performed at the protein elution from the Ni-NTA resin in order to extend the stability of Mistic samples.

The samples for NMR experiments typically contained 0.5 mM either ^{15}N-labeled or ^{13}C/^{15}N-labeled Mistic, 30 mM DPC, 0.2 mM dithiotreitol (DTT), 50 mM KCl, and 10 mM potassium phosphate buffer at pH 6.0.

NMR Experiments

All ^{1}H, ^{15}N, and ^{13}C NMR experiments were performed at 30°C on Bruker Avance 600 or 700 or 800 MHz NMR spectrometers equipped with cryoprobes (Bruker Instruments, Billerica MA). The ^{1}H chemical shifts were referenced to the 2,2-dimethyl-2-silapentene-5-sulfonate resonance at 0 ppm, and the ^{15}N/^{13}C chemical shifts were indirectly referenced. ^{19}F NMR experiments were performed on a Bruker Avance 600 spectrometer with a Bruker TXO probe to determine halothane concentrations in reference to a solution with 10 mM trifluoroacetic acid (TFA). Although the chemical shifts assignments of Mistic in LDAO were done previously[10] and the ^{1}H-^{15}N trosy-HSQC spectra of Mistic in DPC showed high similarity to that in LDAO, we repeated the same 2D and 3D NMR experiments[10] for the ^{13}C and ^{15}N chemical shift assignments of Mistic in DPC. A series of ^{1}H-^{15}N trosy-HSQC spectra were collected on samples with 5 different halothane concentrations, ranging from 0 to 13 mM, to determine site-specific dissociation constants. The CBCA(CO)NH and HBHA(CO)NH spectra were acquired in the absence and presence of halothane so that the chemical shifts of Cα, Cβ, Hα, and Hβ at these two different conditions were obtained for comparison. ^{1}H-^{15}N residual dipolar couplings (RDCs) of Mistic were measured using trosy-IPAP-HSQC pulse sequence with 1024 (^{1}H) × 256 (^{15}N) complex points. The weak alignment of ^{15}N-labeled Mistic in DPC micelles was achieved in both compressed and stretched charged polyacrylamide gel.[12] The degree of alignment for each sample was checked using 1D ^{2}H NMR experiments.

To confirm anesthetic direct interaction with Mistic, ^{1}H saturation transfer difference (STD) [13] NMR was performed on a 0.5 mM ^{15}N-labeled Mistic sample in 30 mM DPC in the presence of 10 mM halothane. As a control, the same experiment was also performed on a similar sample but without Mistic. The spectra were obtained in an interleaved manner using irradiation of 50 ms Gaussian pulses applied on-resonance at 0.58 ppm corresponding to Mistic methyl protons and off-resonance at 40 ppm. The pulse sequence utilized WATERGATE water suppression and spoil sequence to destroy unwanted magnetization.[14] A series of STD spectra were acquired at a range of saturation times: 0.5, 1, 3, 5, 10, 20 and 40 seconds. Each spectrum had 64 scans with a relaxation delay of 40 seconds. The STD ($\Delta I = I_{off} - I_{on}$) was calculated by subtraction of the intensities of on-resonance peak (I_{on}) from off-resonance peak (I_{off}).[15,16]

To characterize the dynamic property of Mistic, spin-lattice (R_1) and spin-spin (R_2) ^{15}N relaxation rate constants were measured with 512 (^{1}H) × 128 (^{15}N) complex points using standard pulse sequences with Echo-Antiecho gradient selection.[17] Nine (ranging from 10–1800 ms) or ten (16–160 ms) variable delays were used for the R_1 or R_2 measurements, respectively. The effective transverse relaxation rate was also measured using relaxation-compensated Carr-Purcell-Meiboom-Gill (CPMG) experiments as a function of CPMG field strength (ν_{CPMG}).[18,19] The ^{15}N R_2 relaxation dispersion data are suited to determine Mistic's conformation exchange on the μs-ms timescale in the presence and absence of halothane. The R_2 relaxation dispersion profiles were recorded at two different magnetic field strengths corresponding to ^{1}H frequencies of 600 and 800 MHz. The experiments were performed in a constant time manner (T_{CP} = 60 ms) on uniformly ^{15}N labeled Mistic samples. The CPMG field strength, ν_{CPMG}, was varied to 33.33, 66.67, 100.00, 133.33, 200.00, 266.67, 333.33, 400.00, 500.00, and 666.67 Hz.

Data Process and Structure Refinement

All NMR data were processed using NMRPipe[20] and analyzed with Sparky.[21] The chemical shift assignments were accomplished with the aid of AutoAssign[22] and manual comparison to the assignments of Mistic in LDAO.[10]

The structure of Mistic in DPC micelles were obtained through refinement of the lowest-energy structures (PDB: 1YGM) of Mistic in LDAO micelles[10] using dihedral angle restraints obtained from Cα and Cβ chemical shift index (CSI)[23] processed using Talos[24] and RDC data of helical regions obtained from two different alignment mediums. The refinement used the slow cooling simulated annealing protocol in Xplor-NIH.[25] The axial (Da) and rhombic (R) components of the alignment tensor in RDC experiments were determined using the histogram method,[26] producing Da = −10.8 and R = 0.23 for samples in compressed gel and Da = −10.0, R = 0.27 for samples in stretched charged gel, respectively. A total of 100 structures were produced in the refinement and half of them with lower energies were used for an averaged structure. The best-fit comparison between experimental RDCs and the refined structures were performed using the program MODULE 1.0.[27]

^{15}N relaxation dispersion data were analyzed using Eq. 1 that encompasses all chemical exchange timescales:[28]

$$R_2(\upsilon_{CPMG}) = \left[R_{20} + (k_{ex}/2) - \upsilon_{CPMG}\cosh^{-1}(D_+\cosh(\eta_+) - D_-\cos(\eta_-))\right] \quad [1]$$

where $D_\pm = 1/2(\pm 1 + (\psi + 2\Delta\omega^2)/(\psi^2 + \xi^2)^{1/2})$, $\eta_\pm = (\upsilon_{CPMG}/2(2)^{1/2})(\pm\psi + (\psi^2 + \xi^2)^{1/2})^{1/2}$, $\psi = k_{ex}^2 - \Delta\omega^2$, $\xi = -2\Delta\omega(p_a k_{ex} - p_b k_{ex})$, and R_{20} is the intrinsic transverse relaxation rates, k_{ex} is the exchange rate, Δω is the difference of chemical shifts between exchange sites *a* and *b*, population of site *a* is denoted by $p_a = (1 - p_b)$, $\nu_{CPMG} = 1/(1\tau)$ and τ is the time between centers of successive 180° pulses in the CPMG pulse sequence.

RESULTS AND DISCUSSION

For increased readability, we present here only the primary results that are intimately related to our discussion and leave other supporting data in the supplemental materials as references.

Halothane Interaction Sites in Mistic

Direct halothane interaction with Mistic was evidenced in the STD experiments based on the nuclear Overhauser effect between bound halothane proton and Mistic protons. As shown in Fig. 1A, halothane signal became observable in STD spectra when the on-resonance saturation frequency was set at 0.58 ppm, a frequency far away from halothane proton but near Hδ of Leu and Ile. The halothane signal in Fig. 1A critically depended on the presence of Mistic. Under the same NMR experimental condition (0.58 ppm for the on-resonance saturation), but without Mistic, there was no observable halothane signal (Fig. 1B), indicating that direct interaction between halothane and Mistic certainly exists. The halothane interacting sites in Mistic were examined by monitoring chemical shift changes of Mistic backbones and sidechains in response to halothane titrations. Fig. 2 shows a representative overlay of Mistic's ^{1}H-^{15}N TROSY-HSQC spectra in the presence and absence of halothane. A number of residues showed profound chemical shift changes after the addition of halothane. Some residues, such as A40 and Q66, had changes not only in their chemical shifts, but also in their signal intensities. After the addition of halothane, the S58 signal became much stronger, but I52 peak intensity became much weaker. The peak intensity signified plausible dynamics alternation in the region where the residue resided. Fig. 3 highlights Mistic residues that experienced obvious changes in chemical shift (HN > 0.05ppm, Cα and Cβ > ±1ppm, Hα and Hβ > ±0.1 ppm) upon halothane

titration. The α2 helix had several residues in the middle of the helix that were sensitive to halothane. The location of residues affected by halothane coincided with the helix kink near A40 and M44, suggesting the possibility that the helical kink acted as a pocket for halothane binding. The chemical shifts of residues in other helices were largely insensitive to anesthetics, except for some residues adjacent to or in loop regions. In contrast to helical residues, all loop residues were more or less perturbed by halothane. These loop residues were located at the micelle head-group region, as evidenced by high sensitivity of their chemical shifts to the head-group changes in micelles from 100% DPC to 40% LDAO/60% DPC (see Fig. 1S in the supplemental materials). Most helical residues or N- and C-terminal residues remained the same chemical shifts when DPC was partially replaced by LDAO, confirming that they were embedded in the micelle hydrocarbon regions or exposed to bulk water.

Halothane dissociation constants in the loop regions were estimated in the range of a few mM (Fig. 2S in the supplemental materials). The observation of halothane attraction to Mistic loop residues at the micelle-water interface is consistent with the notion that general anesthetics prefer amphipathic water-lipid interface.[15,29,30] The significance of this idea lies not only in revealing the nature of anesthetic interaction sites, but also in suggesting potential anesthetic modulation to protein regions at the water-lipid interface that play critical roles in protein functions. Anesthetics could disrupt normal residues' interactions within the same loop or between different loops. Anesthetic disruption on residues interactions between different loops can be more vital. Proper couplings of loop residues in agonist-binding extracellular and transmembrane domains at the water-lipid interface are often crucial for functions of plausible anesthetic targeting channels.[1,2] Modification of interfacial electrostatic interactions by point mutations induced profound changes in channel functions.[31] Because of their preferred interaction with residues at interface, it is conceivable that anesthetics could also affect receptor interfacial interactions and ultimately alter functions of Cys-loop receptors. Such a possibility will be discussed further in the following sections.

The halothane concentration of ~10 mM was suitable for observing halothane effects in our NMR experiments, but one might wonder if this concentration is pharmacologically relevant. A clinically relevant concentration of volatile general anesthetics is often quoted as being in the sub-millimolar (~0.1–1 mM) range. The strict meaning of this range refers to what is measured in saline. For volatile anesthetics administered in patients, the only entity that is constant throughout the body under equilibrium is partial pressure. The concentration in any given compartment depends on the partition coefficient in that compartment. Under the same partial pressure, a 100 μM concentration of halothane in saline translates as ~12 mM concentration in lipids, given a 1:124 saline:lipid partition coefficient of halothane at 30°C.[32] Note that our reported concentration was measured in an excess amount of detergent for stabilizing Mistic. Therefore, the halothane concentration of 10 mM used in our NMR measurements is not as high as it appears and is pharmacologically relevant.

Halothane had Minimal Effects on Mistic Structure

The structure of Mistic in DPC micelles was obtained through refinement of Mistic structure in LDAO[10] using our RDC data attained on Mistic in DPC. We found that Mistic had virtually the same folding in DPC and LDAO. Details of the structure refinement are provided in the supplementary materials (Fig. 3S).

The introduction of halothane to Mistic in DPC did not change the overall structure of Mistic. The chemical shift index (CSI) of Cα, Cβ, and Hα, characterizing the secondary structures of Mistic, were largely unchanged in the absence and presence of 10 mM halothane, especially in helical regions. Fig. 4 displays a comparison of the Cα chemical shift index before (top) and after (bottom) addition of halothane, showing that halothane had a minute impact on the secondary structure of Mistic. Halothane effects on Mistic tertiary structure were determined

via measuring backbone RDCs of Mistic in the absence and presence of 5 mM halothane. The structures of Mistic without and with halothane were both refined using RDC data. Relatively small values of root mean square deviations (RMSDs) of the refined structures in the absence and presence of halothane, as color coded in the Mistic structure in Fig. 5, suggest that the overall tertiary structure of Mistic is well preserved upon addition of halothane.

It was reported previously[15,33,34] that structures of transmembrane peptides remained unchanged in the presence of general anesthetics. Several studies on globular proteins with general anesthetics also found remarkable tolerance of overall protein structures to the added anesthetics at low millimolar concentrations.[9,35–37] Since the folding of Mistic in micelles resembles the structural motif of four transmembrane domains of a subunit in the Cys-loop receptors, the observed structure insensitivity to anesthetic perturbation in the present study may also occur in the Cys-loop receptors. Therefore, it is reasonable to speculate that anesthetic action on those Cys-loop receptors is unlikely via significantly altering receptor structures, though more experimental data should be collected for a final conclusion.

Halothane had Profound Effects on Mistic Motion

Halothane induced changes in Mistic motion were confirmed by at least two lines of experimental evidence. First, some residues showed profound changes in their NMR signal intensities (or line widths) after adding halothane. Secondly, ^{15}N relaxation dispersion experiments indicated that motion on the microsecond-millisecond timescale existed in some regions of Mistic and halothane could alter such motion.

As shown in Fig. 2, residues S58, Q66 and A40 gained higher peak intensities and narrower peak line-widths in the ^{1}H-^{15}N HSQC NMR spectra in the presence of halothane. Several Cα resonance peaks of loop residues S58–L67 also changed from weak to strong after the addition of halothane, as summarized in Fig. 4. In contrary, I52 peak intensity dropped significantly after adding halothane (Fig. 2). These observations could not be adequately explained by the halothane effect on Mistic motion in the picosecond-nanosecond timescale. Changes in longitudinal (R1) and transverse (R2) relaxation rates as well as ^{1}H-^{15}N heteronuclear NOE due to the presence of halothane seem relatively small (see Fig. 4S in the supplemental materials). Intrinsically weak intensity of some NMR peaks could result from conformational-exchange broadening in the μs-ms timescale. The increasing intensity of these peaks after addition of halothane might be the consequence of changes in exchange process,[38] though alternation in peak intensity alone would not provide specific information regarding whether halothane had potentiation or inhibition effect on the exchange.

Quantitative characterization of Mistic's motion on the μs-ms timescale was achieved through ^{15}N R_2 relaxation dispersion measurements. Majority residues of Mistic showed no motion on the μs-ms timescale and their transverse relaxation rates were not affected by a systematical variation of the CPMG field strength, ν_{CPMG}. However, R_2 dispersion dependence on the ν_{CPMG} variation was observed for a number of residues located at the loop connecting α2 and α3 helices (residues S58, D61, Q66, D68), at the loop connecting α1 and α2 helices (residues V29), along helix α2 (T39 and N45), and at the loop connecting α3 and α4 (Y82) helices. Fig. 6 depicts relaxation dispersion profiles for two representative residues, D61 and N45, in the absence and presence of 10 mM halothane. Halothane quenched the exchange contribution to R_2 on residue N45 and suppressed the exchange on D61. This is consistent with the aforementioned increase of peak intensity and decrease of line widths in some residues upon the addition of halothane. The fitting of relaxation dispersion data using Eq. 1 for a two-site (*a* and *b*) exchange model[28] provided estimation of exchange parameters, including differences in chemical shifts between exchanging sites ($\Delta\omega$), the exchange rate (k_{ex}), the relative population of a conformation (p_a or p_b), and the intrinsic transverse relaxation rate (R_{20}) in the absence of chemical exchange. Table 1 summarizes these parameters for several

residues in the absence and presence of 10 mM halothane. The population of the major conformation, p_a was close to, or over, 90% for all these residues and had 0 – 3% increase after the addition of halothane. Δω remained virtually the same for most residues, which is consistent with the aforementioned result that Mistic structure remained the same before and after adding halothane. k_{ex} varied to a different extent on different residues.

Both residues T39 and N45 reside in the middle part of helix α2, where a helical kink occurs in between these two residues. Residue Y82 resides at the end of helix α3. Although these residues experienced the chemical exchange on the μs-ms timescale in the absence of halothane, the exchange disappeared in the presence of halothane, as shown in Table 1. In all these cases, anesthetic halothane suppressed exchange motion. Residue V29 is located at the end of helix α1. Halothane did not completely remove the exchange contribution, but the R_{ex} value of V29 was reduced almost by half and the exchange rate k_{ex} became less than 1/3 of its original value. Residue I52 is located at the end of helix α2. It experienced fast exchange in the absence of halothane (Table 1) and possessed a relatively strong ^{1}H-^{15}N HSQC resonance peak (Fig. 2). However, the resonance peak of I52 virtually vanished due to intermediate exchange induced by halothane. Q66 resides at beginning of helix α3 or end of the loop connecting α2 and α3. The side chain of Q66 is within a few Å of the D61 side chain. Both Q66 and D61 had similar exchange rates that became much slower after the addition of halothane. Interestingly, the α2–α3 loop folds in such a way that S58 at the middle of the loop is not far away from D68, which resides at the beginning of helix α3. The kinetic data also suggest that S58 and D68 share similar exchange rates, and both rates became greater in the presence of halothane. One may wonder if it is possible that these two nearby pairs of residues, Q66 and D61 vs. D68 and S58, have different directions of rate change upon addition of halothane. A close inspection of Mistic structure revealed that both D68 and S58 were oriented inward to helices, while Q66 and D61 were directed outward in the loop and pointed to water phase (see Fig. 5S in the supplementary materials). Distinctive motional characteristics of nearby residues upon ligand binding were also observed previously in SH2 protein.[39]

Several features can be extracted from the ^{15}N relaxation dispersion data presented above. First, residues carrying motion on the μs-ms timescale are often in loop edges or helical ends (V29, I52, Q66, D68, Y82). Second, helical residues are often not involved in slow (μs-ms) dynamics except those (T39 and N45) in helical kink regions. Third, residues far away from each other in primary sequence but close in space (Q66 and D61 vs. D68 and S58) exhibit concerted motion. Last, but most importantly for this study, anesthetic halothane could alter the slow dynamics. Anesthetic molecules could make protein motion faster in one region but slower in another region. The exchange rate (k_{ex}) decreased in most of the aforementioned Mistic residues, but increased in some residues. R_{ex} values of the majority of residues in the presence of halothane were reduced to different degrees, indicating that halothane suppressed motion of these residues on the μs-ms timescale. An opposite effect might also exist. The NMR intensity of residue I52 was severely decreased after adding halothane, indicating an intermediate exchange promoted by halothane. However, a systematic evaluation of the slow dynamics of I52 in the presence of 10 mM halothane was prohibited by the weak signal of this residue.

We want to point out that the aforementioned dynamical changes due to the addition of halothane may not necessarily result from direct halothane interaction with individual residues. Most of the residues listed in Table 1 showed obvious chemical shifts in response to halothane titration. However, neither I52 nor Y82 demonstrated significant changes in their chemical shifts, suggesting that these two residues had no close interaction with halothane molecules. The dynamical alternation of these residues must result from halothane allosteric modulation. Therefore, anesthetic molecules could induce changes in protein motions on the μs-ms

timescale either through direct interaction with specific residues or through allosteric modulation.

CONCLUSIONS

The most significant contribution of the present study is providing unequivocal experimental evidence that inhaled general anesthetics can modulate protein slow dynamics, especially motion in the flexible loops that link different alpha helices. Protein motion is essential for protein functions. It is well known that protein motion on the microsecond-millisecond timescale often couples with protein functions.[40] Low affinity drugs, such as volatile general anesthetics, do not usually interact with proteins in a lock-and-key fashion.[41] Therefore, it is rational for us to determine how anesthetics alter protein functions via altering protein motion. Our previous computational studies established a theoretical basis for anesthetic action on protein global dynamics.[3,4] Experimental evidence is critical for validating the theory of anesthetic action on protein dynamics. Our study demonstrates that halothane perturbed Mistic slows dynamics, which indicates a plausibility that changes in protein functions by general anesthetic can be achieved through interrupting mode of protein motion[4] instead of tight bindings with number of protein hydrophobic pockets. These findings on Mistic certainly encourage us to look further into anesthetic effects on protein motion in other functional proteins. By collecting enough experimental data demonstrating anesthetic modulation on protein dynamics, we can significantly advance our understanding of molecular mechanisms of general anesthesia.

Identification of the halothane interaction sites on Mistic in this study support our view that anesthetics prefer to interact with amphipathic sites of proteins.[7,15,29,30] Although halothane interaction occurred at multiple sites of Mistic, it did not introduce significant secondary and tertiary structure changes. This observation is consistent with our previous findings on other proteins.[15,29,34]

One may wonder if the anesthetic effects, such as those observed here on Mistic, are large enough to account for anesthetic action on proteins. Because of the low affinity nature of inhaled general anesthetics (submillimolar), their interaction with proteins should not be expected to cause structural and dynamical effects on proteins as great as those high affinity ligands or substrates. We are still in the process of determining how large an anesthetic effect on protein structures and dynamics is required to produce protein functional changes that ultimately contribute to general anesthesia. Experiments on model proteins are only the starting point of this process. The demonstration of halothane perturbation to dynamics of Mistic in the μs-ms timescale is such a starting point.

Halothane perturbation on Mistic slow dynamics happened not only to residues that might interact directly with halothane molecules, but also to residues that seemed to be remote from halothane, signifying halothane allosteric modulation on protein dynamics. It is conceivable that the impact of general anesthetic modulation on protein dynamics, be it direct or indirect through allosteric effects, will be amplified on much larger protein complexes, such as Cys-loop receptors, in which the concerted motion among different subunits regulates the protein functions. Normally several different conformers of these protein complexes coexist dynamically and each conformer determines different functional states. Anesthetic perturbation in a few critical sites could introduce vital disturbance to highly coupled motion in these molecular machineries, shift the equilibrium of conformational states, and ultimately alter protein functions. When a large enough number of proteins in the central nervous system (CNS) are dynamically perturbed by general anesthetics, even though the perturbation on individual proteins is rather small, the accumulating effects on the CNS could lead to the phenomena of general anesthesia. The study on Mistic provides encouraging evidence for

pursuing a dynamical view of molecular mechanisms of general anesthesia. Further investigation on other proteins is necessary to confirm that anesthetic modulation to functionally important motion in proteins contributes to general anesthesia.

Supplementary Material

Refer to Web version on PubMed Central for supplementary material.

ACKNOWLEDGEMENT

The authors would like to thank Prof. Rieko Ishima for the stimulating discussions and her input into the application of the R_2 dispersion relaxation all-timescale fitting program. The assistance from Dr. Tommy S. Tillman in Mistic expression, Ms. Nicole Brandon in gel preparations for RDC measurements, and Mrs. Sandra C. Hirsch in manuscript editing is highly appreciated. This work was supported in part by grants from the National Institute of Health (R01GM56257 and R01GM66358 to P.T. and R37GM049202 to Y.X.).

REFERENCES

1. Franks NP, Lieb WR. Nature 1984;310:599. [PubMed: 6462249]
2. Campagna JA, Miller KW, Forman SA. N Engl J Med 2003;348:2110. [PubMed: 12761368]
3. Tang P, Xu Y. Proc Natl Acad Sci U S A 2002;99:16035. [PubMed: 12438684]
4. Szarecka A, Xu Y, Tang P. Biophys. J 2007;93:1895. [PubMed: 17513367]
5. Mihic SJ, Ye Q, Wick MJ, Koltchine VV, Krasowski MD, Finn SE, Mascia MP, Valenzuela CF, Hanson KK, Greenblatt EP, Harris RA, Harrison NL. Nature 1997;389:385. [PubMed: 9311780]
6. Johansson JS, Gibney BR, Rabanal F, Reddy KS, Dutton PL. Biochemistry 1998;37:1421. [PubMed: 9477971]
7. Cui T, Bondarenko V, Ma D, Canlas C, Brandon NR, Johansson JS, Xu Y, Tang P. Biophys J 2008;94:4464. [PubMed: 18310239]
8. Ma D, Brandon NR, Cui T, Bondarenko V, Canlas C, Johansson JS, Tang P, Xu Y. Biophys J 2008;94:4454. [PubMed: 18310240]
9. Liu R, Loll PJ, Eckenhoff RG. Faseb J 2005;19:567. [PubMed: 15791007]
10. Roosild TP, Greenwald J, Vega M, Castronovo S, Riek R, Choe S. Science 2005;307:1317. [PubMed: 15731457]
11. Marley J, Lu M, Bracken C. J Biomol NMR 2001;20:71. [PubMed: 11430757]
12. Cierpicki T, Bushweller JH. J Am Chem Soc 2004;126:16259. [PubMed: 15584763]
13. Moriz Mayer BM. Angewandte Chemie International Edition 1999;38:1784.
14. Hwang TL, Shaka AJ. Journal of Magnetic Resonance, Series A 1995;112:275.
15. Bondarenko V, Yushmanov VE, Xu Y, Tang P. Biophys. J 2008;94:1681. [PubMed: 17993502]
16. Streiff JH, Juranic NO, Macura SI, Warner DO, Jones KA, Perkins WJ. Mol Pharmacol 2004;66:929. [PubMed: 15385643]
17. Farrow NA, Muhandiram R, Singer AU, Pascal SM, Kay CM, Gish G, Shoelson SE, Pawson T, Forman-Kay JD, Kay LE. Biochemistry 1994;33:5984. [PubMed: 7514039]
18. Tollinger M, Skrynnikov NR, Mulder FA, Forman-Kay JD, Kay LE. J Am Chem Soc 2001;123:11341. [PubMed: 11707108]
19. Loria JP, Rance M, Palmer AG. J. Am. Chem. Soc 1999;121:2331.
20. Delaglio F, Grzesiek S, Vuister GW, Zhu G, Pfeifer J, Bax A. J Biomol NMR 1995;6:277. [PubMed: 8520220]
21. Goddard, TD.; Kneller, DG. San Francisco: University of California;
22. Zimmerman DE, Kulikowski CA, Huang Y, Feng W, Tashiro M, Shimotakahara S, Chien C, Powers R, Montelione GT. J Mol Biol 1997;269:592. [PubMed: 9217263]
23. Wishart DS, Sykes BD, Richards FM. J Mol Biol 1991;222:311. [PubMed: 1960729]
24. Cornilescu G, Delaglio F, Bax A. J Biomol NMR 1999;13:289. [PubMed: 10212987]

25. Schwieters CD, Kuszewski JJ, Tjandra N, Clore GM. J Magn Reson 2003;160:65. [PubMed: 12565051]
26. Clore GM, Gronenborn AM, Bax A. J Magn Reson 1998;133:216. [PubMed: 9654491]
27. Dosset P, Hus JC, Marion D, Blackledge M. J Biomol NMR 2001;20:223. [PubMed: 11519746]
28. Carver JP, Richards RE. Journal of Magnetic Resonance (1969) 1972;6:89.
29. Tang P, Simplaceanu V, Xu Y. Biophys J 1999;76:2346. [PubMed: 10233053]
30. Xu Y, Tang P. Biochim Biophys Acta 1997;1323:154. [PubMed: 9030222]
31. Kash TL, Jenkins A, Kelley JC, Trudell JR, Harrison NL. Nature 2003;421:272. [PubMed: 12529644]
32. Smith RA, Porter EG, Miller KW. Biochim Biophys Acta 1981;645:327. [PubMed: 7272292]
33. Tang P, Hu J, Liachenko S, Xu Y. Biophys J 1999;77:739. [PubMed: 10423422]
34. Tang P, Mandal PK, Zegarra M. Biophys J 2002;83:1413. [PubMed: 12202367]
35. Kruse SW, Zhao R, Smith DP, Jones DN. Nat Struct Biol 2003;10:694. [PubMed: 12881720]
36. Colloc'h N, Sopkova-de Oliveira Santos J, Retailleau P, Vivares D, Bonnete F, Langlois d'Estainto B, Gallois B, Brisson A, Risso JJ, Lemaire M, Prange T, Abraini JH. Biophys J 2007;92:217. [PubMed: 17028130]
37. Franks NP, Jenkins A, Conti E, Lieb WR, Brick P. Biophys J 1998;75:2205. [PubMed: 9788915]
38. Rao BD. Methods Enzymol 1989;176:279. [PubMed: 2811690]
39. Mittag T, Schaffhausen B, Gunther UL. Biochemistry 2003;42:11128. [PubMed: 14503863]
40. Ishima R, Torchia DA. Nat Struct Biol 2000;7:740. [PubMed: 10966641]
41. Xu Y, Seto T, Tang P, Firestone L. Biophys J 2000;78:746. [PubMed: 10653787]

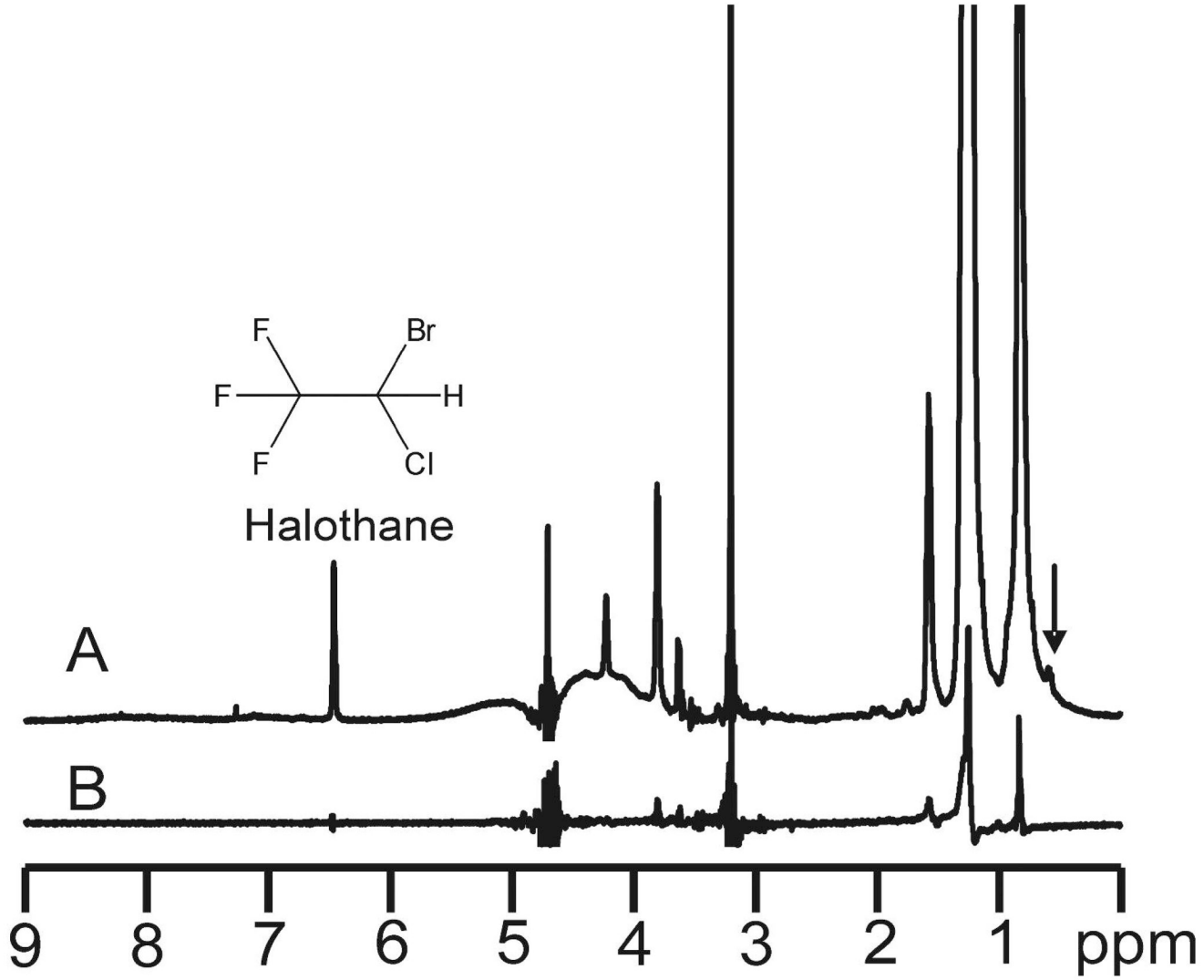

Figure 1.

^{1}H saturation-transfer difference (STD) NMR spectra of 10 mM halothane (resonance at 6.48 ppm) in (A) 30 mM DPC with 0.5 mM Mistic; (B) 50 mM DPC without Mistic. The arrow indicates the frequency for on-resonance saturation at 0.58 ppm that is near Hδ resonance of Leu and Ile residues in Mistic. Note that halothane signal was not observed in (B) under the same NMR condition as in (A) but without Mistic, indicating the direct interaction between halothane and Mistic. A stick chemical structure of halothane is inserted for reference.

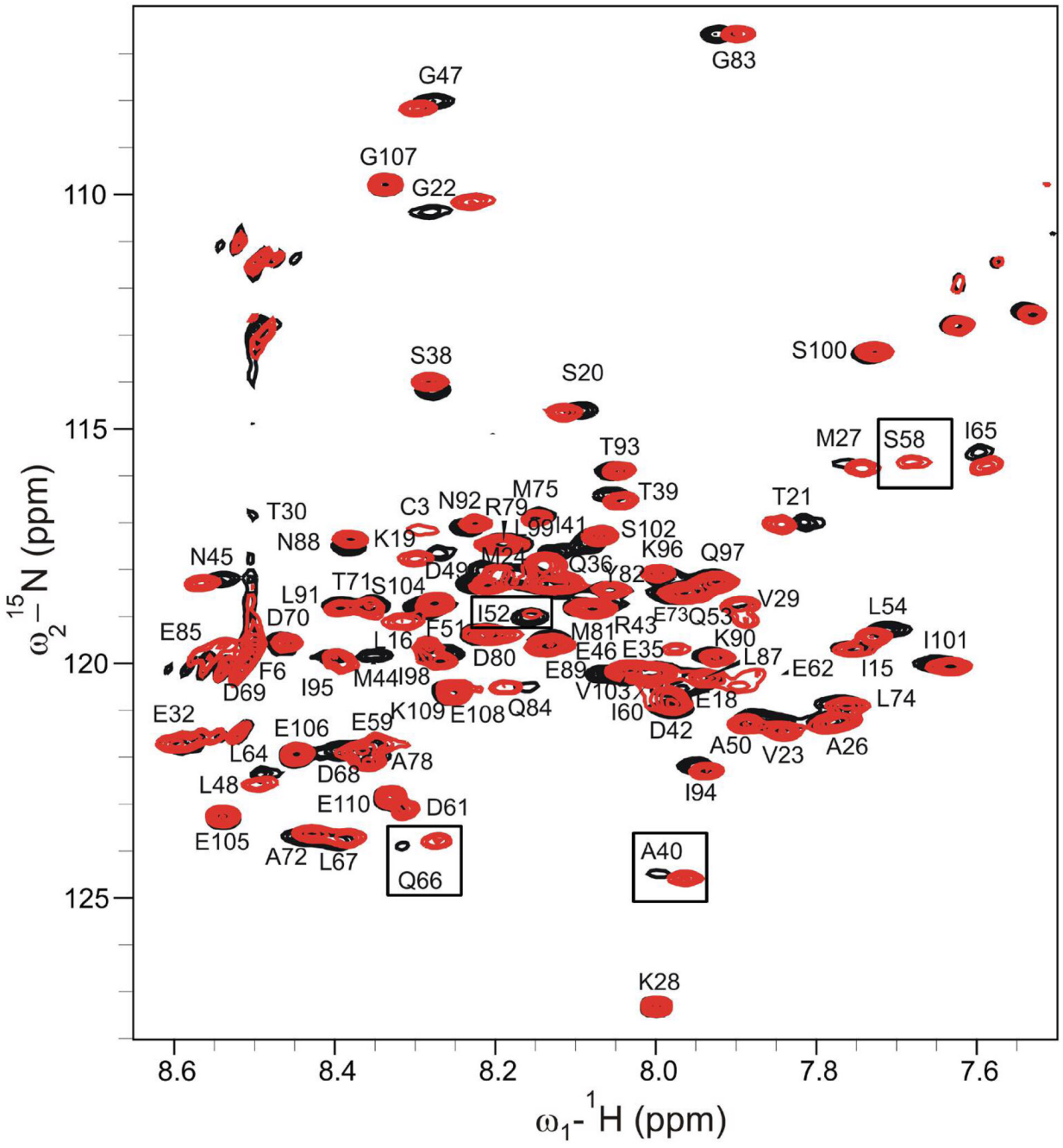

Figure 2.

Overlay of ^{1}H-^{15}N TROSY-HSQC spectra of 0.5 mM Mistic in 30 mM DPC micelles in the absence (black) and presence (red) of 10 mM halothane. The spectra were acquired at 30°C. Despite many residues were undisturbed by the addition of halothane, some residues experienced significant chemical shift changes and/or intensity changes of their resonance signals. A few examples are highlighted in small boxes.

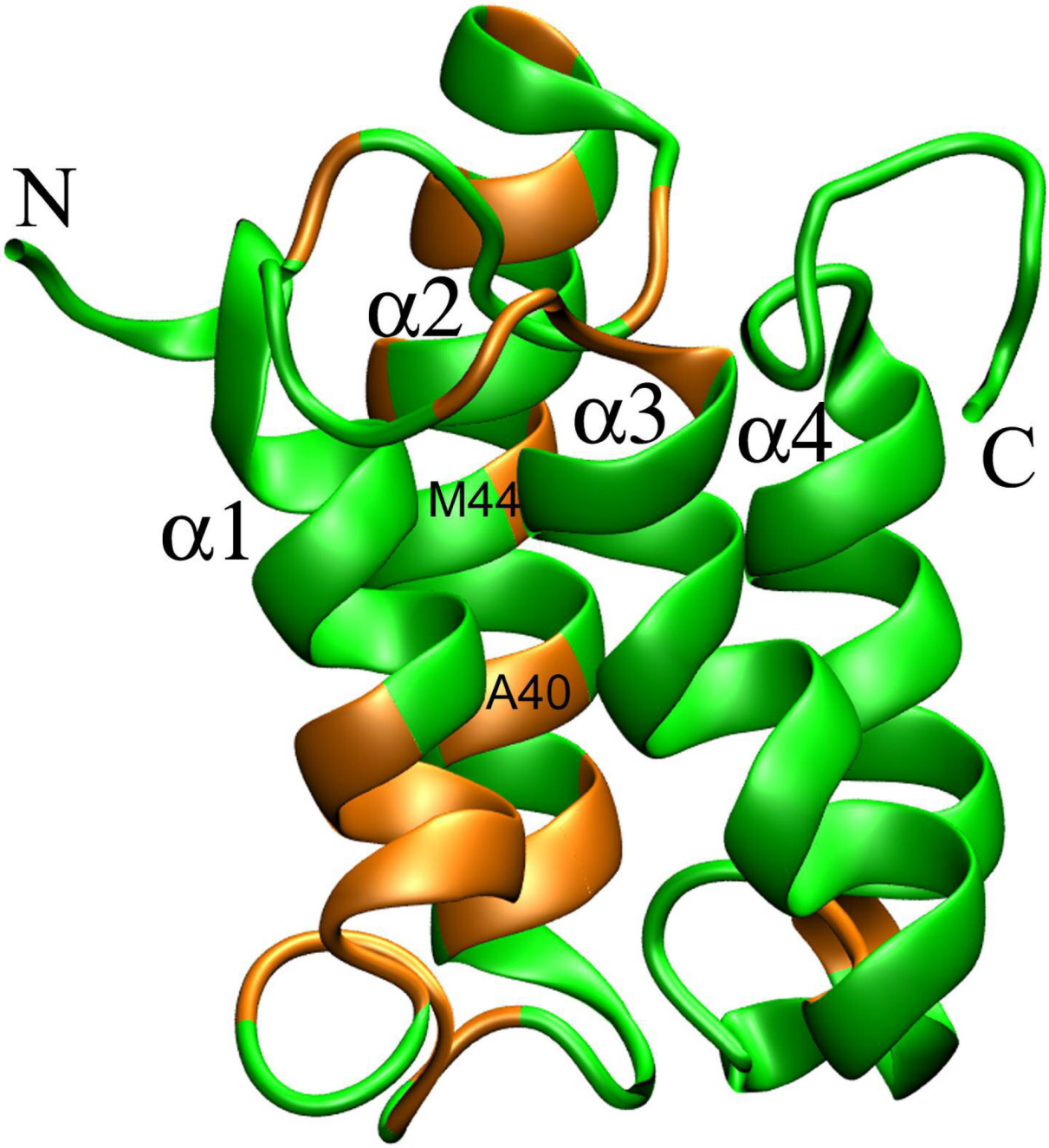

Figure 3.
Halothane interaction sites in Mistic. The residues whose chemical shifts were significantly perturbed by halothane are highlighted in orange color. The four transmembrane helices are marked as α1–α4.

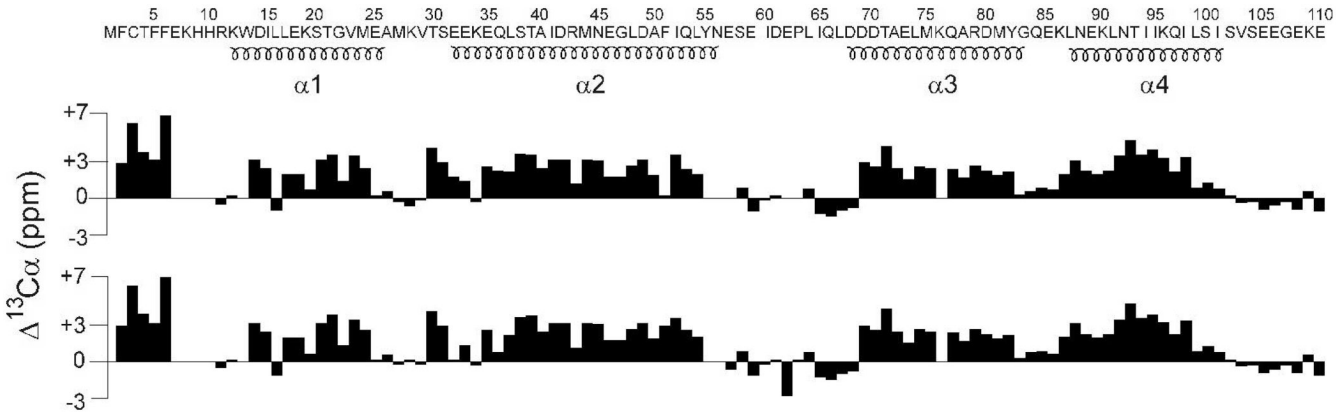

Figure 4.

The ^{13}Ca chemical shift index of Mistic residues in the absence (top) and presence (bottom) of 10 mM halothane. The Cα chemical shifts were referenced with respect to random coil values at 0 ppm.

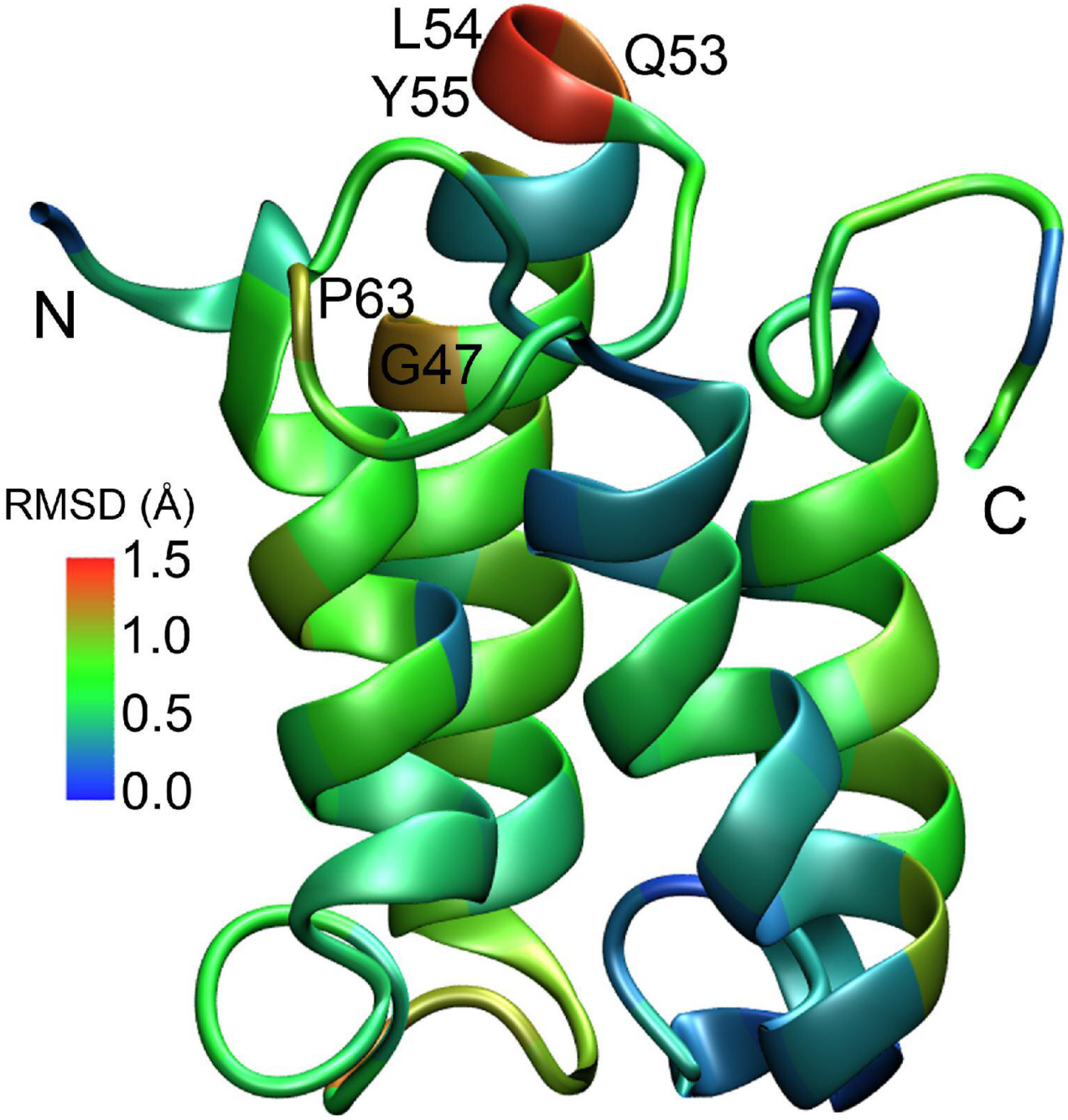

Figure 5.
The refined structure of Mistic in DPC on the basis of RDC NMR measurements. The RMSD (Å) of Mistic structure in the absence and presence of 10 mM halothane is presented using a color scale. Residues that showed largest RMSD are labeled.

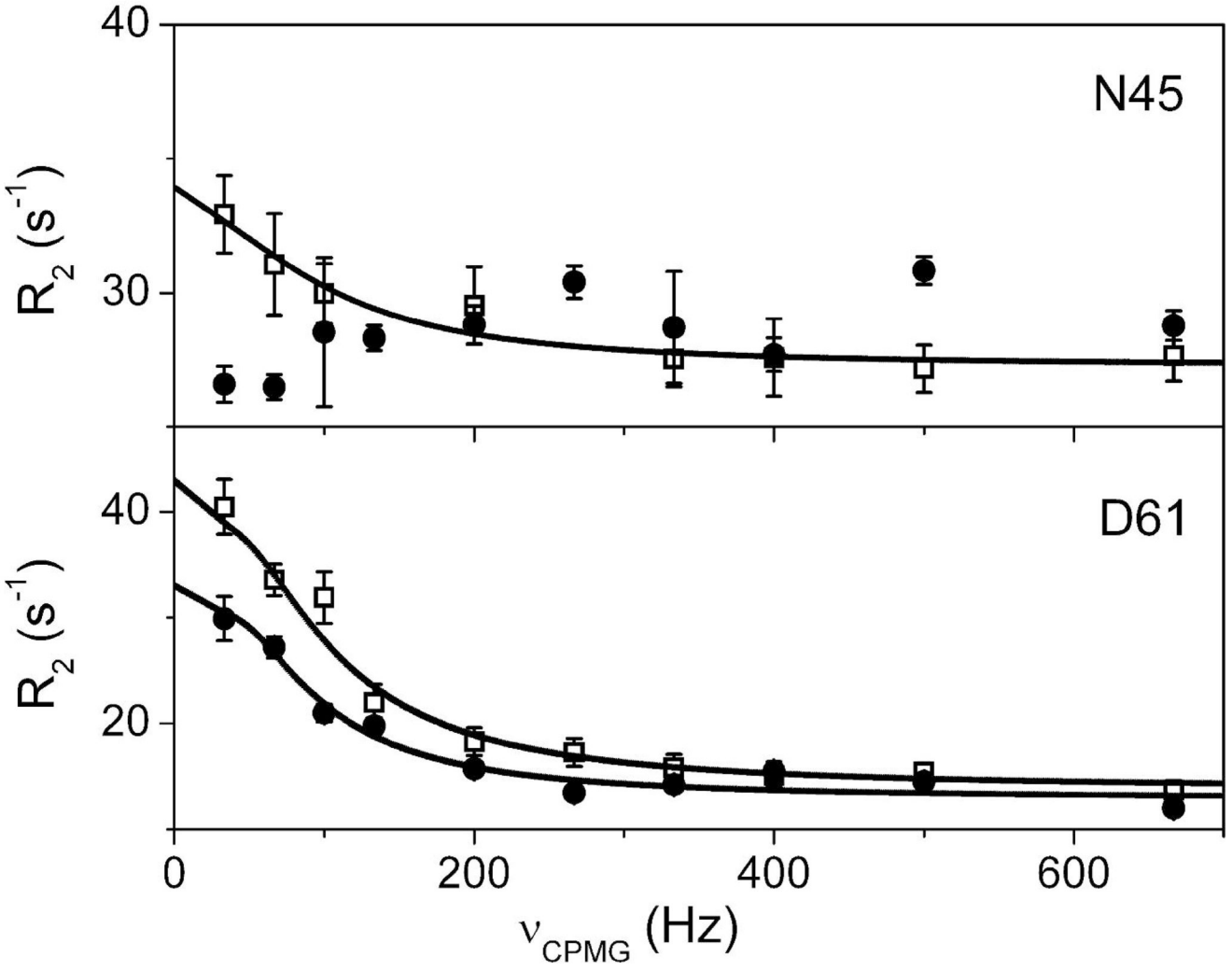

Figure 6.
Backbone ^{15}N relaxation dispersion curves of two representative Mistic residues, N45 and D61, in the absence (□) and presence (•) of 10 mM halothane.

Table 1

^{15}N Relaxation Dispersion Parameters[a] of Exchanging Residues of Mistic in the absence and presence of 10 mM halothane

Residues	Absence (−) & Presence (+) of Halothane	R_{ex} (s^{-1})[b]	R_{20} (s^{-1})	k_{ex} (s^{-1})	p_a	Δw (s^{-1})
V29	−	7.8	16.4 ± 0.7	532 ± 290	0.97 ± 0.02	508 ± 59
	+	4.2	16.9 ± 0.2	154 ± 22	0.97 ± 0.02	523 ± 69
T39	−	3.9	20.7 ± 0.3	1455 ± 296	0.98 ± 0.08	588 ± 65
	+	NA				
N45	−	5.2	27.3 ± 0.4	635 ± 197	0.92 ± 0.02	258 ± 28
	+	NA				
I52	−	6.2	23.7 ± 0.4	722 ± 200	0.90 ± 0.02	241 ± 30
	+	ND				
S58	−	6.4	15.8 ± 0.3	217 ± 83	0.91 ± 0.03	205 ± 12.5
	+	4.8	17.2 ± 0.5	551 ± 270	0.91 ± 0.03	189 ± 33
D61	−	26.7	13.5 ± 0.9	468 ± 144	0.89 ± 0.02	529 ± 26
	+	17.9	13.2 ± 0.5	199 ± 22	0.90 ± 0.01	550 ± 50
Q66	−	12.9	17.0 ± 0.7	376 ± 99	0.90 ± 0.03	362 ± 18
	+	12.0	17.1 ± 0.6	174 ± 33	0.92 ± 0.01	486 ± 74
D68	−	3.5	17.9 ± 0.2	279 ± 120	0.97 ± 0.02	317 ± 25
	+	3.3	16.3 ± 0.1	482 ± 84	0.97 ± 0.02	300 ± 15
Y82	−	11.5	25.0 ± 1.1	267 ± 148	0.87 ± 0.17	244 ± 24
	+	NA				

[a] Equation 1 was used for fitting of these parameters.

[b] $R_{ex} = R_2(\nu_{cp} \rightarrow 0) - R_2(\nu_{cp} \rightarrow \infty)$

NA: no relaxation dispersion

ND: the signal was too weak to determine relaxation dispersion parameters